

UPCommons

Portal del coneixement obert de la UPC

<http://upcommons.upc.edu/e-prints>

Aquesta és una còpia de la versió *author's final draft* d'un article publicat a la revista *Acta geophysica*.

La publicació final està disponible a Springer a través de <http://dx.doi.org/10.1007/s11600-018-0126-1>

This is a copy of the author 's final draft version of an article published in *Acta geophysica*.

The final publication is available at Springer via <http://dx.doi.org/10.1007/s11600-018-0126-1>

Article publicat / Published article:

Pérez Zanón, N. [et al.] (2018) Analysis of synoptic patterns in relationship with severe rainfall events in the Ebre Observatory (Catalonia). *Acta geophysica*. Doi: 10.1007/s11600-018-0126-1



Analysis of synoptic patterns in relationship with severe rainfall events in the Ebre Observatory (Catalonia)

Núria Pérez-Zanón¹ · M. Carmen Casas-Castillo² · Juan Carlos Peña³ · Montserrat Aran³ · Raúl Rodríguez-Solà⁴ · Angel Redaño⁵ · German Solé⁶

Received: 30 November 2017 / Accepted: 9 March 2018
© Institute of Geophysics, Polish Academy of Sciences & Polish Academy of Sciences 2018

Abstract

The study has obtained a classification of the synoptic patterns associated with a selection of extreme rain episodes registered in the Ebre Observatory between 1905 and 2003, showing a return period of not less than 10 years for any duration from 5 min to 24 h. These episodes had been previously classified in four rainfall intensity groups attending to their meteorological time scale. The synoptic patterns related to every group have been obtained applying a multivariable analysis to three atmospheric levels: sea-level pressure, temperature, and geopotential at 500 hPa. Usually, the synoptic patterns associated with intense rain in southern Catalonia are featured by low-pressure systems advecting warm and wet air from the Mediterranean Sea at the low levels of the troposphere. The configuration in the middle levels of the troposphere is dominated by negative anomalies of geopotential, indicating the presence of a low or a cold front, and temperature anomalies, promoting the destabilization of the atmosphere. These configurations promote the occurrence of severe convective events due to the difference of temperature between the low and medium levels of troposphere and the contribution of humidity in the lowest levels of the atmosphere.

Keywords Synoptic patterns · Severe rainfall · Southern Catalonia · Meteorological temporal scales · Intensity weighted index · Multivariate analysis

Introduction

Overview

In mid-latitude Mediterranean areas, intense rain is usually produced by intense convective systems, often embedded in larger low-pressure structures, with a particular organization highly affected by seasonal and local factors. In the specific case of Catalonia, located in the northeast of the Iberian Peninsula, with an intricate topography delimited in the north by the Pyrenees range and in the east by the Mediterranean Sea and the Prelitoral Range, the proximity of the sea is one of the most relevant factors (Fig. 1).

To investigate the trigger factors of a meteorological extreme rain situation, both the spatial and time rain organization must be analyzed by studying the association between the maximum amounts recorded in different temporal intervals for the same rain episode (Lorente and Redaño 1990; Casas et al. 2004). Thus, an objective classification of the intense rainfall episodes can be carried out

- ✉ Núria Pérez-Zanón
nuria.perez@urv.cat
- Centre for Climate Change (C3), University Rovira i Virgili, Campus Terres de l'Ebre, Av. Remolins, 13-15, 43500 Tortosa, Tarragona, Spain
 - Departament de Física, ESEIAAT, Universitat Politècnica de Catalunya BarcelonaTech (UPC), Colom 1, 08222 Terrassa, Spain
 - Servei Meteorològic de Catalunya, Berlín, 38-46, 08029 Barcelona, Spain
 - Departament de Física, ETSEIB, Universitat Politècnica de Catalunya BarcelonaTech (UPC), Diagonal 647, 08028 Barcelona, Spain
 - Departament de Física Aplicada, Facultat de Física, Universitat de Barcelona (UB), Martí i Franqués, 1, 08028 Barcelona, Spain
 - Observatori de l'Ebre, Terra Alta, 38, 43520 Roquetes, Spain

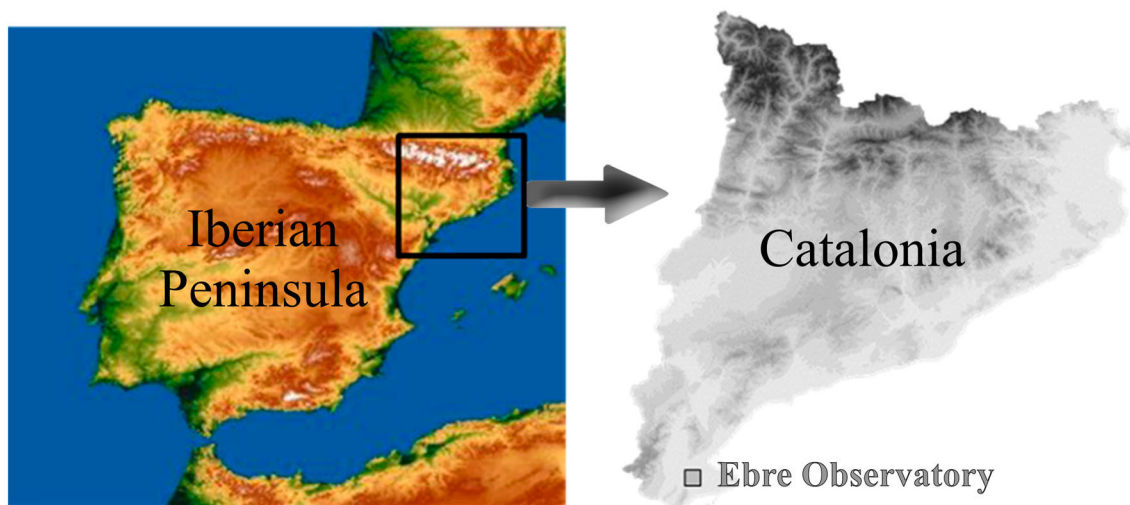


Fig. 1 Geographical location of the Ebre Observatory

41 in base of their different temporal organizations. Some
 42 studies obtained classifications of extreme rain events
 43 registered at several locations of the Eastern seaside area of
 44 Catalonia, as Casas et al. (2004, 2010) who analyzed a
 45 selection of intense storms registered in the Fabra Obser-
 46 vatory of Barcelona between 1927 and 1992 by a Jardí
 47 gauge, and by the urban rain gauge network of this city
 48 between 1994 and 2001, and Pérez-Zanón et al. (2015) who
 49 obtained the classification of severe storms from an almost
 50 centennial rainfall register (1905–2003) of the Ebre
 51 Observatory near Tortosa (Tarragona). In both cases, the
 52 selected storms resulted classified by cluster analysis in
 53 four groups, attending on their temporal characteristics:
 54 microscale, mesoscale, synoptic scale, and a fourth group
 55 of complex events. This last group showed high rainfall
 56 rates for a large temporal range associated with phenomena
 57 of different scales acting together, for instance, mesoscale
 58 organizations embedded into synoptic systems, situation
 59 that usually produce extremely intense rainfall and occa-
 60 sionally flooding.

61 The degree of severity or exceptionality of an extreme
 62 rainfall event is usually quantified in terms of the total
 63 amount of water collected in a given period of time. Thus,
 64 this period of time is commonly chosen depending on the
 65 geomorphological characteristics of the catchment area to
 66 determine, for instance, the time of concentration and
 67 response to exceptional rainfall in this particular area.
 68 Casas et al. (2004) suggested an intensity weighted index
 69 (IP) to establish an objective method of classification based
 70 on the rain amounts exceptionality for four representative
 71 durations of the characteristic scales of atmospheric
 72 motion: 5 min, 1, 2, and 24 h, representing microscale
 73 weather phenomena, meso- γ , meso- β , and synoptic scale,
 74 respectively (Thunis and Bornstein 1996). This index IP is

useful to provide a single measure of the rainfall severity
 from a meteorological point of view, regardless of the
 consequences in a particular type of watershed. The index
 IP was applied by Pérez-Zanón et al. (2015) to quantify the
 degree of exceptionality of the high intense episodes
 recorded in the Ebre Observatory.

Multivariate analysis techniques are extensively used to
 find relationships between atmospheric circulation patterns
 and exceptional meteorological events, such as very intense
 rain (Vicente-Serrano et al. 2009; Martínez et al. 2008;
 Martín-Vide et al. 2008; Houssos et al. 2008). A method-
 ology based on cluster analysis (CA) and principal com-
 ponent analysis (PCA) was employed by Peña et al. (2011)
 to get a catalogue of synoptic patterns to explain the strong
 wind episodes in Catalonia, and by Aran et al. (2011) to
 characterize the typical meteorological conditions produc-
 ing hailstorms on the inland Catalanian area of the Lleida
 plain. In the present work, this methodology has been
 applied to the selection of exceptional storms registered in
 the Ebre Observatory between 1905 and 2003, to identify
 the synoptic patterns contributing to the generation of such
 extreme rainfall events in this area.

Previous work

Rainfall data used in this study were obtained from the
 digitalized records of two siphon gauges situated in the
 Ebre Observatory (Fig. 2) between 1905 and 2003, with an
 interruption from April 4, 1938, to May 1, 1939 due to the
 Spanish civil war.

After a frequency analysis performed on the maximum
 rain amounts for 16 different durations (5, 10, 15, 20, 25,
 30, 35, 40, 45, 50, 55, and 60 min, and 2, 6, 12, and 24 h),
 Pérez-Zanón et al. (2015) calculated the intensity–



Fig. 2 Location of recording rain gauges at the Ebre Observatory

107 duration–frequency (IDF) curves for the Ebre Observatory.
 108 According to those IDF curves, Pérez-Zanón et al. (2015)
 109 analyzed and classified a selection of 28 rainfall events
 110 with amounts exceeding the ID curve corresponding to
 111 10 years of return period for any of the considered time
 112 intervals.

113 These 28 selected events were studied by Pérez-Zanón
 114 et al. (2015) to analyze the prevailing meteorological time
 115 scales involved and were classified using a cluster analysis
 116 in four Rainfall Intensity Groups (RIG): a first group (I) of
 117 microscale or highly local episodes, with a clear diurnal
 118 cycle and seasonal influence, a second group (II) of the
 119 events showing intense rainfall for mesoscale durations, a
 120 third group (III) of synoptic rainfall events, and a fourth
 121 group (IV) of complex episodes showing high intensities
 122 for a large time range, indicating that different scale
 123 meteorological processes have contributed together to
 124 produce precipitation. The values of the IP index measur-
 125 ing the degree of complexity of these events were also
 126 calculated.

127 Objective of the present work

128 The aim of the present study is to obtain a classification of
 129 the synoptic patterns related to extreme rain events regis-
 130 tered in the Ebre Observatory (1905–2003) taking their
 131 meteorological time scales into consideration to better
 132 understand high intense rainfall intensity events in the
 133 south of Catalonia and their possible forecasting in the
 134 future. By applying multivariate analysis, it is desired to
 135 obtain the synoptic patterns associated with these extreme
 136 events and study their link to the four RIG groups (I, II, III,
 137 and IV) to characterize the prevailing meteorological
 138 conditions favouring the different kind of heavy rainfall
 139 episodes in the area.

140 Compared to similar studies, the present work is pro-
 141 viding two novelties: the first is related to the identification

of the precipitation episode according to its meteorological
 time scale, while the second is the methodology followed
 to obtain the synoptic patterns; a multivariate analysis
 taking into account the main dynamic and thermodynamic
 atmospheric processes giving rise to rainfall.

Data

For the 28 extreme episodes with a return period not less
 than 10 years for any duration from 5 min to 24 h regis-
 tered in the Ebre Observatory between 1905 and 2003
 (Pérez-Zanón et al. 2015), the synoptic patterns were
 determined from the daily grids of the mean sea-level
 pressure (SLP), temperature at 500 hPa (T_{500}) and geop-
 ontential at 500 hPa (Z_{500}), obtained from the twentieth
 century V2 Reanalysis Project (20CRP, Compo et al.
 2011), extending the time coverage of the NCEP/NCAR
 Reanalysis Project (Kalnay et al. 1996). The 20CRP pro-
 duces reanalyzes of weather maps with a horizontal spatial
 resolution of 2° from 1871 onwards.

Methods

The synoptic patterns have been obtained by a multivari-
 able analysis based on three steps: PCA, CA, and dis-
 criminant analysis (DA), applied to three atmospheric
 levels (SLP, T_{500} , and Z_{500}) to detect the principal dynamic
 and thermodynamic atmospheric processes (Fig. 3). The
 variables employed are the daily anomalies of SLP, Z_{500} ,
 and T_{500} (aSLP, a Z_{500} , and a T_{500}), corrected each grid point
 by the squared root of the latitude.

Principal component analysis

The use of PCA for classifying synoptic patterns is twofold
 (Huth et al. 2008). In our analysis, PCA has been employed
 for the reduction of the variables dimension. This proce-
 dure has been performed on every third data set by the use

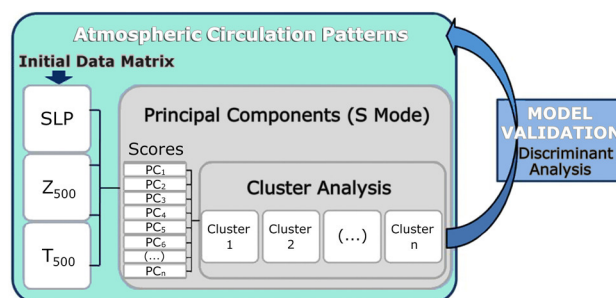


Fig. 3 Scheme of the different multivariable analysis methodologies applied

174 of an S-mode data matrix, with grid points as variables and
 175 observations as days. Both the correlation matrix and the
 176 Scree test have been employed to identify the principal
 177 components (Huth 1996; Cattell 1966). The Orthogonal
 178 Varimax procedure has been applied to rotate the compo-
 179 nents for minimizing the number of variables which have
 180 high factorial loadings (Richman 1986).

181 Cluster analysis

182 The main synoptic patterns in relationship with heavy
 183 rainfall were detected using the non-hierarchical K-means
 184 technique performed on the matrix built by the individual
 185 factor scores matrix resulting from the PCA. For using this
 186 algorithm, the number of groups to obtain has to be defined
 187 beforehand. Despite different techniques were developed
 188 for other authors (Tibshirani et al. 2001; Ain 2010; Debatty
 189 et al. 2014), the election of the number clusters is still quite
 190 subjective. For this study, the “elbow method” was
 191 applied, which is based in choosing a number clusters, so
 192 that adding another cluster, the data would not be signifi-
 193 cantly better explained. Different parameters could be used
 194 to decide the number of initial clusters: the variance
 195 explained by clusters against the number of clusters
 196 (Thorndike 1953) or, the selected parameter for the present
 197 study, sum of squares (SSD) within clusters (Aran et al.
 198 2011; Zhang 2016).

199 To determine the proper number of clusters to classify
 200 the extreme rain events spatial configuration, the next steps
 201 have been followed. First, the SSD for different number of
 202 clusters (from 1 to 28 in this case) considered are obtained
 203 by applying Ward method. The Ward method is similar to
 204 K-means (minimize SSD); however, it does not need a
 205 initial number of clusters. The graphical representation of
 206 SSD in front of the number of cluster considered allows to
 207 apply the elbow method to select the number of clusters: it
 208 corresponds to the position in which the highest change in
 209 the slope is found. This number of clusters will be initially
 210 used on the K-means to define the groups (Aran et al.
 211 2011).

212 Discriminant analysis

213 DA has been applied as a validation of the model and for
 214 re-classifying the bordering events (Michailidou et al.
 215 2009). Since predefined classes are needed to perform a
 216 categorization by DA (Sioutas and Flocas 2003), the pre-
 217 vious classification obtained from CA has been taken into
 218 account. Thus, the CA step has been used as a predictor for
 219 DA, that is, a CA specific group has been assigned to each
 220 day of the factor scores matrix of DA. Then, the discrim-
 221 inant functions, useful to re-classify new data, have been

obtained by applying the Wilks’ lambda criterion (Diab
 et al. 1991).

Synoptic patterns related to RIG composites

To characterize the spatial configuration of the state of the
 atmosphere for each RIG, composites have been obtained.
 Thus, the mean value of each grid point has been computed
 for the days belonging to each RIG for SLP, T_{500} , and Z_{500} .
 The spatial configuration of the synoptic patterns and the
 composites has been compared by the Pearson Product
 Moment correlation coefficient applied to SLP fields.

Results

The synoptic patterns characterizing the atmosphere during
 the 28 extreme rainfall events have been obtained. The
 PCA applied to individual variables gives a reduction of
 seven components to explain SLP, nine in the case of T_{500} ,
 and six for Z_{500} . From the CA, seven clusters have been
 determined as the number of clusters necessities to char-
 acterize the state of the atmosphere during these events.
 However, when applying DA, the number of clusters
 decreases to 5 due to the redistribution of the events in the
 group: at the beginning (after DA), the number of clusters
 were 6 (8) in the synoptic type 1, 1 (0) in the synoptic type
 2, 2 (2) in type 3, 11 (12) in type 4, 5 (4) in type 5, 2 (2) in
 type 6, and 1 (0) in synoptic type 7. Thus, synoptic type 2
 and 7, which originally had 1 event, disappeared.

After determining RIG composites, the correlation
 analysis was computed between them and the synoptic
 patterns (see Table 1 and Figs. 4, 5, 6, 7, 8). The highest
 correlation for RIG I is 0.89 with synoptic type 4. As it was
 described by Pérez-Zanón et al. (2015), this group is
 indicative of highly local or microscale rain episodes,
 characteristics of the late summer and fall with a clear
 diurnal surface heating effect involved in their convective
 development, since all them occurred after midday. The IP
 is low–medium index for this group, with values less than

Table 1 Correlation coefficients of Pearson between the composites of the Rainfall Intensity Group (RIG) and the synoptic patterns computed from the multivariable analysis

RIG	IP range	Synoptic pattern	Correlation
I	0.55–0.80	4	0.89
IIA	0.64–0.86	5	0.91
IIB	0.74–1.02	6	0.77
III	0.48–0.75	3	0.33
IV	1.26–1.62	1	0.79

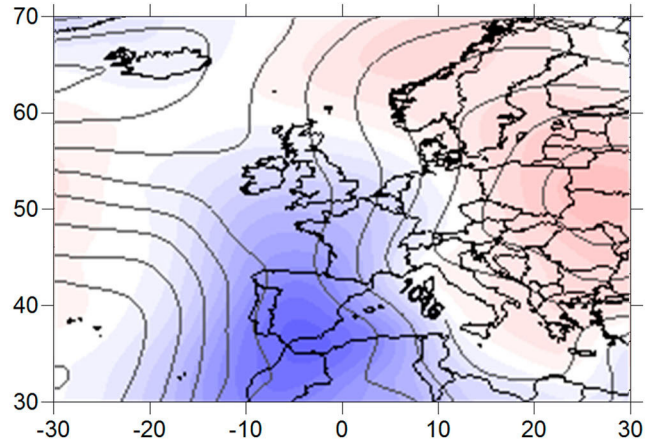
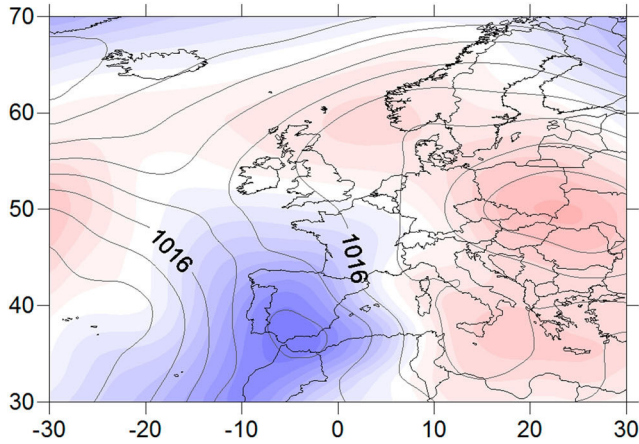


Fig. 4 Composites of RIG I (left) and the maximum correlated synoptic type 4 (right). Lines represent SLP (hPa), while colored areas are aSLP with blue (red) colors represent negative (positive)

anomalies. The synoptic configuration promotes precipitation in south Catalonia due to the SE flux linked to pressure and geopotential negative anomalies over the west of the Iberian Peninsula

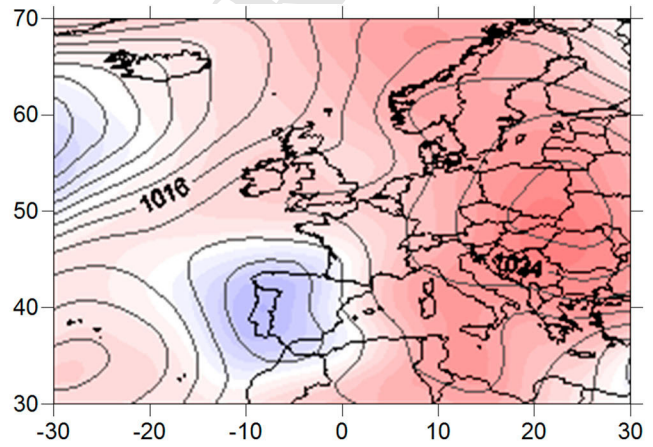
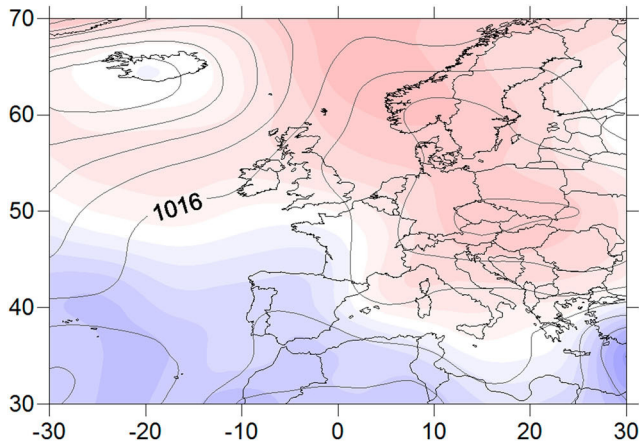


Fig. 5 Composites of RIG IIA (left) and the maximum correlated synoptic type 5 (right). Lines represent SLP (hPa), while colored areas are aSLP with blue (red) colors represent negative (positive)

anomalies. The synoptic configuration is related to the cut-off low-pressure system with cold air in the middle levels of the troposphere promoting instability and the occurrence of severe thunderstorms

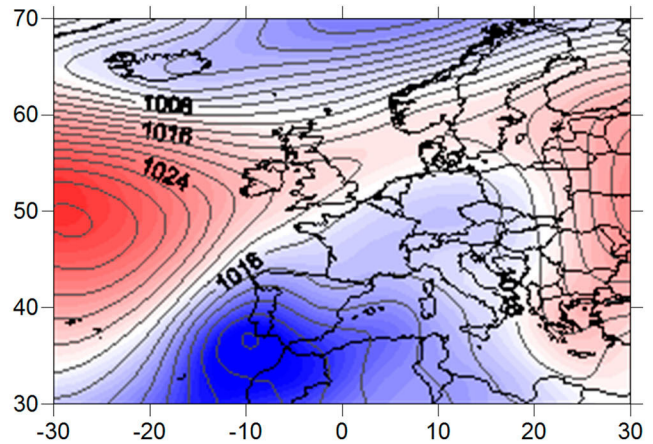
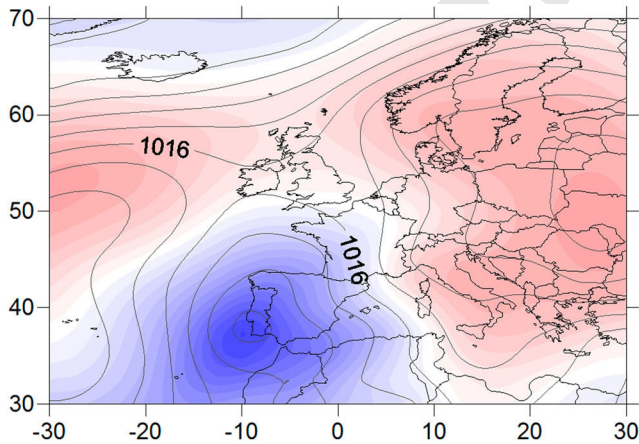


Fig. 6 Composites of RIG IIB (left) and the maximum correlated synoptic type 6 (right). Lines represent SLP (hPa), while colored areas are aSLP with blue (red) colors represent negative (positive)

anomalies. The synoptic configuration promotes precipitation in south Catalonia due to the east flux linked to pressure and geopotential negative anomalies over the Mediterranean area

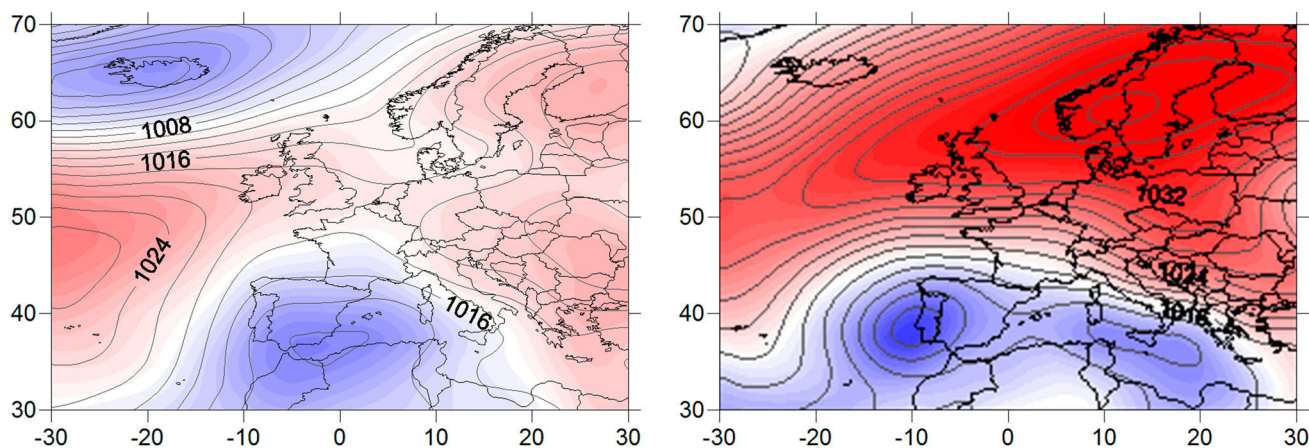


Fig. 7 Composites of RIG III (left) and the maximum correlated synoptic type 3 (right). Lines represent SLP (hPa), while colored areas are aSLP with blue (red) colors represent negative (positive)

anomalies. The synoptic configuration promotes precipitation in south Catalonia due to the east flux linked to pressure and geopotential negative anomalies over the Mediterranean area

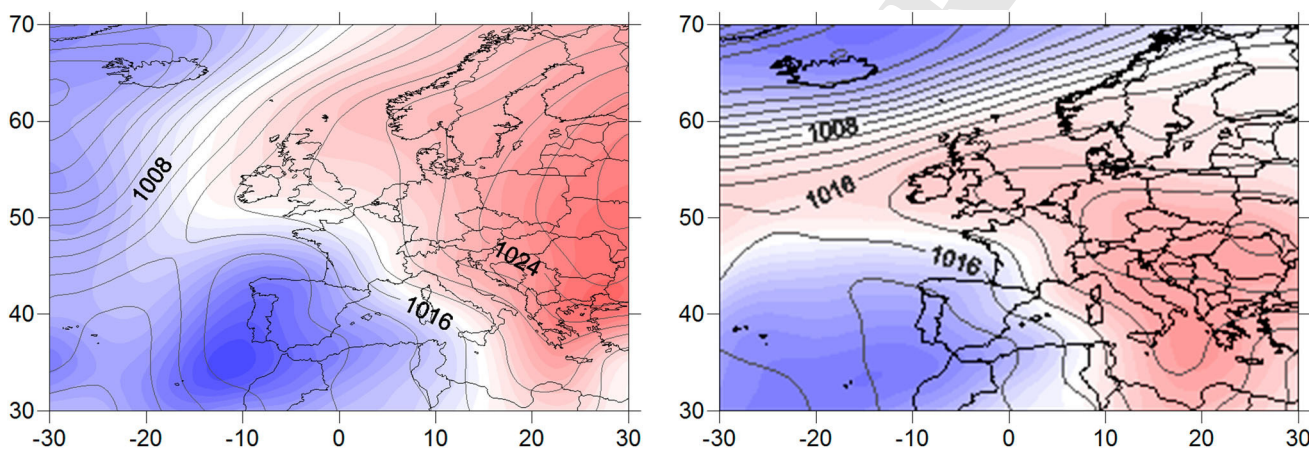


Fig. 8 Composites of RIG IV (left) and the maximum correlated synoptic type 1 (right). Lines represent SLP (hPa), while colored areas are aSLP with blue (red) colors represent negative (positive)

anomalies. The synoptic configuration promotes precipitation in south Catalonia due to the SE flux linked to pressure and geopotential negative anomalies over the Iberian Peninsula

257 1. The synoptic configuration promotes the precipitation in
258 Catalonia due to the south-east flux linked with pressure
259 and geopotential negative anomalies over the west of the
260 Iberian Peninsula. The conjunction of wet and warm low
261 flow from the Mediterranean Sea with cold air in the
262 middle levels of the troposphere promotes atmospheric
263 instability and the occurrence of thunderstorms.

264 The maximum correlation of RIG IIA has been 0.91
265 with synoptic type 5. The four events grouped as IIA
266 showed high intensities until 35–60 min and were identified
267 by Pérez-Zanón et al. (2015) as meso- γ -scale convective
268 systems, at the edge of microscale. The IP is
269 medium index, with values between 0.64 and 0.86. The
270 synoptic configuration promotes the precipitation in Catalonia
271 due to the south flow linked with pressure and geopotential
272 negative anomalies over the Iberian Peninsula.
273 The cut-off low-pressure system with cold air in middle

levels promotes instability and the occurrence of severe
thunderstorms.

The second division of group II, as it also characterizes
mesoscale phenomena, RIG IIB has maximum correlation
(0.77) with synoptic type 6. It presents high intensities for
12–24 h what is linked to meso- α and meso- β scales,
typically in relationship with very dynamic Atlantic fronts
moving slowly with strong mesoscale rain systems
embedded (Pérez-Zanón et al. 2015). The IP shows a
medium–high index, with values between 0.74 and 1.02.
The synoptic configuration promotes the precipitation in
Catalonia due to the east flow linked with pressure and
geopotential negative anomalies over the Mediterranean
area. The intense flow of east or south-eastern linked to this
configuration with the anomalies of geopotential and temperature
in middle levels stimulates intense thunderstorms,

290 and a stagnation of this situation can cause long-lasting
291 rainfall episodes.

292 RIG III, which shows a maximum correlation of 0.33
293 with synoptic type 3, corresponds to synoptic rain events,
294 whose intensity is higher than the 10-year return period
295 level for durations longer than 9 h. In this case, the IP is a
296 low index, with values between 0.48 and 0.75. The syn-
297 optic configuration promotes the precipitation in Catalonia
298 due to the east flow linked with pressure and geopotential
299 negative anomalies over the Mediterranean area. The flow
300 of east linked to this configuration with the anomalies of
301 geopotential and temperature in the middle levels of the
302 troposphere provoke rainfall in Catalonia: advective and
303 long-largest rainfall with low intensities.

304 Finally, the RIG IV has a correlation of 0.79 with syn-
305 optic type 1. This RIG is associated with the most intricate
306 storms, showing the combined action of processes corre-
307 sponding to several meteorological scales. This kind of
308 complex events is usually constituted by synoptic situa-
309 tions causing large-scale rain simultaneously to mesoscale
310 convective systems producing extremely intense rainfall,
311 with even embedded smaller convective cells. These epi-
312 sodes are the main cause of flooding in the area. The IP
313 shows a high index, with values between 1.26 and 1.62.
314 The synoptic configuration promotes the precipitation in
315 Catalonia due to the south-east flow linked with pressure
316 and geopotential negative anomalies over the Iberian
317 Peninsula. The flow of south-east (warm and wet) provokes
318 long-lasting rainfall in Catalonia. This rainfall may be both
319 convective due to the high degree of the tropospheric
320 instability and advective due to the anticyclonic blocking,
321 which prevents the progress of the low-pressure center to
322 the east.

323 Discussion

324 Regarding similar studies, the analysis made provides two
325 novelties: the first is related to the identification of the
326 extreme precipitation episodes, while the second is the
327 methodology to obtain the synoptic patterns associated
328 with.

329 A precipitation event is usually defined as extreme when
330 it exceeds a certain threshold of cumulative precipitation.
331 However, different criteria are used to define this threshold
332 (for more information, see Merino et al. 2017). In the
333 present study, a return period of 10 years was used as
334 threshold in the selection of the extreme rainfall episodes
335 registered in the Ebre Observatory between 1905 and 2003
336 (Pérez-Zanón et al. 2015), classified in RIGs after taken
337 into consideration their meteorological time scales. Then,
338 the multivariate analysis in three steps (PCA, CA, and DA)
339 has been carried out to obtain the specific synoptic patterns

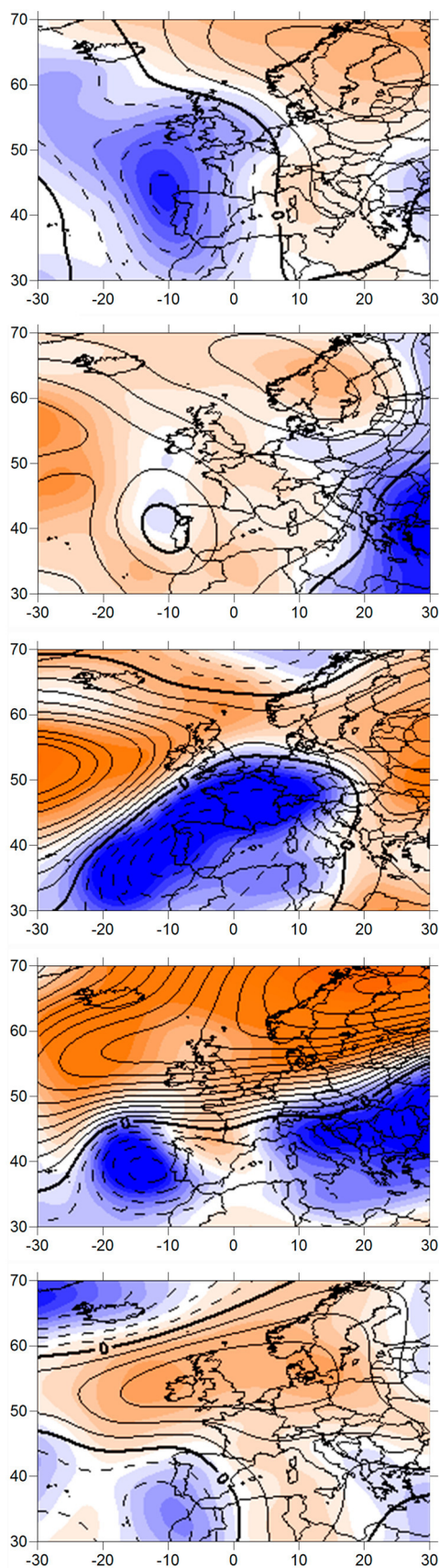
340 associated with the RIGs. This analysis has been performed
341 on three atmospheric levels (SLP, T_{500} , and Z_{500}) to detect
342 the principal dynamic and thermodynamic atmospheric
343 processes related to intense rainfall generation. Further-
344 more, this technique can be used to re-classify new data
345 (Aran et al. 2011; Peña et al. 2011).

346 The results show that the methodology used has been
347 useful to obtain the synoptic patterns related to the four
348 RIG groups (I, II, III, and IV), to better understand high
349 intense rain intensity episodes in the south of Catalonia and
350 their forecasting in the future. The prevailing synoptic
351 conditions that favour heavy rainfall in this area have
352 shown a good correspondence with the RIG classification.

353 The synoptic patterns are characterized by low-pressure
354 systems that interact with the Mediterranean warm-air
355 mass promoting the destabilization the atmosphere. The
356 atmospheric configuration in Z_{500} (Fig. 9) is dominated by
357 negative anomalies of geopotential and temperature,
358 showing the presence of a low-pressure center or an
359 Atlantic cold front (Casas et al. 2004, 2010; Pérez-Zanón
360 et al. 2015). These types of configurations enhance the
361 occurrence of convective events due to the difference of
362 temperature between T_{500} and T_{850} (warm air from the
363 Mediterranean Sea and negative anomalies of temperature
364 in middle levels) and the humidity input in the lowest
365 levels of the atmosphere. Furthermore, the presence of a
366 high-pressure system over Europe can provoke a stagnation
367 of the synoptic situation causing long-lasting rain over the
368 studied area.

369 Two different types of heavy rain can affect the lower
370 part of the Ebre basin (Merino et al. 2017): (1) advective
371 precipitations during winter and spring with low or med-
372 ium convectivity linked to a zonal disposition of the syn-
373 optic configuration, producing heavy accumulated
374 precipitation over several days and (2) the extremely con-
375 vective summer and autumn storms are linked to the
376 cyclones that become more intense over the Mediterranean
377 Sea, producing long-lasting and intense rain due to the
378 Mediterranean warm-air mass, the orographic uplift of the
379 air mass, and the instability produced by negative anoma-
380 lies of geopotential height at the middle levels of the tro-
381 posphere (Peña et al. 2015).

382 Flood represents a high natural hazard for mid-latitude
383 Mediterranean regions (Llasat et al. 2013); therefore, the
384 precipitation rate behaviour must be contemplated for
385 designing hydraulic works, and evaluate natural risk due to
386 eventual extreme rain events (Casas et al. 2004, 2010;
387 Beguería et al. 2011; Pérez-Zanón et al. 2015; Merino et al.
388 2017; Rodríguez-Solà et al. 2017). Particularly, in the south
389 of Catalonia, heavy precipitation is normally connected
390 with peak discharges measured in Tortosa (MAGRAMA
391 2015), located in the lower part of the Ebre basin, near of
392 Ebre Observatory (Ruiz-Bellet et al. 2015). Two types of



◀**Fig. 9** Composites of the synoptic patterns 4, 5, 6, 3, and 1 (up to down) for 500 hPa. Lines represents ΔZ_{500} (m) and colored areas are ΔT_{500} (0°C) with blue (red) colors represent negative (positive) anomalies

behaviour within the flood series are detected in several 393
analyses (Mazon et al. 2014; Ruiz-Bellet et al. 2015; Pino 394
et al. 2016). The differences are linked to the two types of 395
rainstorms. A more frequent behaviour related to flat-peak 396
discharges might be caused by winter and spring advective 397
rainfall of low or medium convectivity, while a less fre- 398
quent one associated with high-peak discharges might be 399
caused by highly convective summer and autumn storms. 400
Therefore, extreme hydrological events in the Ebre basin 401
seem to be controlled by the atmospheric dynamics acting 402
both in the Mediterranean area (high-convectivity rainfall) 403
and in the North Atlantic (long-lasting and advective 404
rainfall). The most important flood events are a combina- 405
tion of the two atmospheric process and is related to the 406
RIG group number IV ($IP > 1.25$). The main characteris- 407
tics of the synoptic patterns corresponding to this complex 408
rain episodes (14% of the investigated cases) are the 409
existence of an Atlantic depression at the south-west of the 410
Iberian Peninsula and a strong blocking anticyclone over 411
Europe (Casas et al. 2004, 2010; Pérez-Zanón et al. 2015). 412
In these situations, there is usually a moist and warm 413
advective flow from the Mediterranean Sea, since the 414
predominant wind over Catalonia is from the south-east 415
both at 850 hPa and on the surface. These atmospheric 416
configurations cause long-lasting advective rain while 417
simultaneously convective phenomena associated with the 418
south-east warm flow in low levels produce extremely 419
intense precipitation (Peña et al. 2015; Pérez-Zanón et al. 420
2015). 421

It is important to remark that trends of extreme rainfall 422
records over the twenty-first century are nowadays one of 423
the most interesting topics in climate change studies 424
(Beguería et al. 2011). The spatial and time analysis of 425
precipitation data is a relevant research for a better 426
understanding and prevention of the possible effects of 427
climate change in rainfall extremes. 428

Conclusions 429

The multivariate analyses have been a success to identify 430
the main features to detect of the main dynamic and ther- 431
modynamic atmospheric processes. The synoptic patterns, 432
which characterize the origin of the extreme rainfall in the 433
Observatori de l'Ebre, have been found by a multivariate 434
analysis applied independently to three atmospheric vari- 435
ables over the European sector. Therefore, the synoptic 436

437 patterns, in addition to being able to characterize the spatial
438 configuration of the atmosphere, capture differences in the
439 intensity and temporal distribution at local scale of the rain.

440 The synoptic patterns associated with severe rain in
441 southern Catalonia are featured by low-pressure systems
442 advecting wet and warm air from the Mediterranean Sea in
443 the low levels of the atmosphere. The most predominant
444 flow is from south-east, followed by the east. The config-
445 uration in the middle levels of the troposphere is dominated
446 by negative anomalies of geopotential, indicating the
447 presence of a low or a cold front, and temperature
448 anomalies, promoting the destabilization of the atmo-
449 sphere. These types of configurations promote the occur-
450 rence of severe convective events due to the difference of
451 temperature between the two levels analyzed (warm air
452 from the Mediterranean Sea and negative anomalies of
453 temperature at middle levels) and the humidity contribution
454 in the lowest levels. Furthermore, the presence of a
455 blocking high-pressure system over Europe can cause the
456 stagnation of the synoptic configuration and produce long-
457 lasting precipitation.

458 **Acknowledgements** We are grateful to the Meteorological Service of
459 Catalonia, the Ebre Observatory, the DOE INCITE project, BER and
460 NOAA.

461 Compliance with ethical standards

462 **Conflict of interest** On behalf of all authors, the corresponding author
463 states that there is no conflict of interest.

464 References

- 465 Aran M, Peña JC, Torà M (2011) Atmospheric circulation patterns
466 associated with hail events in Lleida (Catalonia). *Atmos Res*
467 100(4):428–438. <https://doi.org/10.1016/j.atmosres.2010.10.029>
- 468 Beguería S, Angulo-Martínez M, Vicente-Serrano SM, López-
469 Moreno JL, El-Kenawy A (2011) Assessing trends in extreme
470 precipitation events intensity and magnitude using non-station-
471 ary peaks-over-threshold analysis: a case study in northeast
472 Spain from 1930 to 2006. *Int J Climatol* 31:2102–2114. <https://doi.org/10.1002/joc.2218>
- 473 Casas MC, Codina B, Redaño A, Lorente J (2004) A methodology to
474 classify extreme rainfall events in the western Mediterranean
475 area. *Theor Appl Climatol* 77:139–150. <https://doi.org/10.1007/s00704-003-0003-x>
- 476 Casas MC, Rodríguez R, Redaño A (2010) Analysis of extreme
477 rainfall in Barcelona using a microscale rain gauge network.
478 *Meteorol Appl* 17:117–123. <https://doi.org/10.1002/met.166>
- 479 Cattell RB (1966) The scree test for the number of the factors.
480 *Multivar Behav Res* 1:245–276
- 481 Compo GP, Whitaker JS, Sardeshmukh PD, Matsui N, Allan RJ, Yin
482 X, Gleason BE, Vose RS, Rutledge G, Bessemoulin P, Brönni-
483 mann S, Brunet M, Crouthamel RI, Grant AN, Groisman PY,
484 Jones PD, Kruk MC, Kruger AC, Marshall GJ, Maugeri M, Mok
485 HY, Nordli Ø, Ross TF, Trigo RM, Wang XL, Woodruff SD,
486 Worley SJ (2011) The twentieth century reanalysis project. *Q J R*
487 *Meteorol Soc* 137:1–28. <https://doi.org/10.1002/qj.776>

- 490 Debatty T, Michiardi P, Mees W, Thonnard O (2014) Determining the
491 k in k-means with MapReduce. *EDBT/ICDT Workshops*,
492 pp 19–28
- 493 Diab RD, Preston-Whyte RA, Washington R (1991) Distribution of
494 rainfall by synoptic type over Natal, South Africa. *Int J Climatol*
495 11(8):877–888
- 496 Fernandez GC (2002) Discriminant analysis, a powerful classification
497 technique in data mining. In: *Proceedings of the SAS users* 97
498 international conference, pp 247–256
- 499 Huth R (1996) Properties of the circulation classification
500 scheme based on the rotated principal component analysis.
501 *Meteorol Atmos Phys* 59:217–233
- 502 Huth R, Beck C, Philipp A, Demuzere M, Ustrnul Z, Cahynová M,
503 Kyselý J, Tveito OE (2008) Classifications of atmospheric
504 circulation patterns. Recent advances and applications. trends
505 and directions in climate research. *Ann N Y Acad Sci*
506 1146:105–152. <https://doi.org/10.1196/annals.1446.019>
- 507 Jain AK (2010) Data clustering: 50 years beyond K-means. *Pattern*
508 *Recognit Lett* 31(8):651–666
- 509 Kalnay E, Kanamitsu M, Kistler R, Collins W, Deaven D, Gandin L,
510 Iredell M, Saha S, White G, Woollen J, Zhu Y, Leetmaa A,
511 Reynolds B, Chelliah M, Ebisuzaki W, Higgins W, Janowiak J,
512 Mo KC, Ropelewski C, Wang J, Jenne R, Joseph D (1996) The
513 NCEP/NCAR 40-year reanalysis project. *Bull Am Meteorol Soc*
514 77(3):437–472. [https://doi.org/10.1175/1520-0477\(1996\)077<0437:tnyrp>2.0.co;2](https://doi.org/10.1175/1520-0477(1996)077<0437:tnyrp>2.0.co;2)
- 515 Llasat MC, Llasat-Botija M, Petrucci O, Pasqua AA, Rossello J, Vinet
516 F, Boissier L (2013) Towards a database on societal impact of
517 Mediterranean floods within the framework of the HYMEX
518 project. *Nat Hazards Earth Syst Sci* 13(5):1337–1350. <https://doi.org/10.5194/nhess-13-1337-013>
- 519 Lorente J, Redaño A (1990) Rainfall rate distribution in a local scale:
520 the case of Barcelona City. *Theor Appl Climatol* 41:23–32.
521 <https://doi.org/10.1007/BF00866199>
- 522 MAGRAMA (2015) Ministerio de Agricultura, Alimentación y
523 Medio Ambiente: Anuario de aforos. <http://sig.magrama.es/aforos/visor.html>. Accessed: 18 Nov 2015
- 524 Martín-Vide J, Sánchez-Lorenzo A, López-Bustins JA, Cordobilla
525 MJ, García-Manuel A, Raso JM (2008) Torrential rainfall in
526 northeast of the Iberian Peninsula: synoptic patterns and WeMO
527 influence. *Adv Sci Res* 2:99–105
- 528 Mazon J, Balasch JC, Barriendos M, Ruiz-Bellet JL, Pino D, Tuset J
529 (2014) Meteorological reconstruction of major floods in early
530 instrumental period in Catalonia (NE Iberian Peninsula). In:
531 EMS annual meeting abstracts, 11, EMS2014–141
- 532 Merino A, Fernández-González S, García-Ortega E, Sánchez JL,
533 López L, Gascón E (2017) Temporal continuity of extreme
534 precipitation events using sub-daily precipitation: application to
535 floods in the Ebro basin, northeastern Spain. *Int J Climatol*.
536 <https://doi.org/10.1002/joc.5302>
- 537 Michailidou C, Maheras P, Arseni-Papadimitriou A, Kolyva-
538 Machera F, Anagnostopoulou C (2009) A study of weather
539 types at Athens and Thessaloniki and their relationship to
540 circulation types for the cold-wet period, part II: discriminant
541 analysis. *Theor Appl Climatol* 97(1–2):179–194
- 542 Peña JC, Aran M, Cunillera J, Amaro J (2011) Atmospheric
543 circulation patterns associated with strong wind events in
544 Catalonia. *Nat Hazards Earth Syst Sci* 11:145–155. <https://doi.org/10.5194/nhess-11-145-2011>
- 545 Peña JC, Schulte L, Badoux A, Barriendos M, Barrera-Escoda A
546 (2015) Influence of solar forcing, climate variability and
547 atmospheric circulation patterns on summer floods in Switzer-
548 land. *Hydrol Earth Syst Sci Discuss* 11:13843–13890. <https://doi.org/10.5194/hessd-11-13843-2014>
- 549 Pérez-Zanón N, Casas-Castillo MC, Rodríguez-Solà R, Peña JC, Rius
550 A, Solé JG, Redaño A (2015) Analysis of extreme rainfall in the
551

- 556 Ebre Observatory (Spain). *Theor Appl Climatol* 573
 557 124(3–4):935–944. <https://doi.org/10.1007/s00704-015-1476-0> 574
 558 Pino D, Ruiz-Bellet JL, Balasch JC, Romero-León L, Tuset J, 575
 559 Barriendos M, Mazon J, Castellort X (2016) Meteorological and 576
 560 hydrological analysis of major floods in NE Iberian Peninsula. 577
 561 *J Hydrol* 541:63–89. <https://doi.org/10.1016/j.jhydrol.2016.02.008> 578
 562 579
 563 Richman MB (1986) Rotation of principal components. *J Climatol* 580
 564 6:293–335 581
 565 Rodríguez-Solà R, Casas-Castillo MC, Navarro X, Redaño A (2017) 582
 566 A study of the scaling properties of rainfall in Spain and its 583
 567 appropriateness to generate intensity-duration-frequency curves 584
 568 from daily records. *Int J Climatol* 37(2):770–780. <https://doi.org/10.1002/joc.4738>. <http://hdl.handle.net/2117/87312> 585
 569 586
 570 Ruiz-Bellet JL, Balasch JC, Tuset J, Monserrate A, Sánchez A (2015) 587
 571 Improvement of flood frequency analysis with historical infor- 588
 572 mation in different types of catchments and data series within the 589
 Ebro River basin (NE Iberian Peninsula). *Z Geomorphol Suppl Issues* 59(3):127–157. https://doi.org/10.1127/zfg_suppl/2015/S-59219 590
 Sioutas MV, Flocas HA (2003) Hailstorms in Northern Greece: 591
 synoptic patterns and thermodynamic environment. *Theor Appl Climatol* 75:189–202 592
 Thorndike RL (1953) Who belongs in the family? *Psychometrika* 18(4):267–276 593
 Thunis P, Bornstein R (1996) Hierarchy of mesoscale flow assumptions and equations. *J Atmos Sci* 53(3):380–397. [https://doi.org/10.1175/1520-0469\(1996\)053](https://doi.org/10.1175/1520-0469(1996)053) 594
 Tibshirani R, Walther G, Hastie T (2001) Estimating the number of clusters in a data set via the gap statistic. *J R Stat Soc Ser B (Stat Methodol)* 63(2):411–423 595

UNCORRECTED PROOF